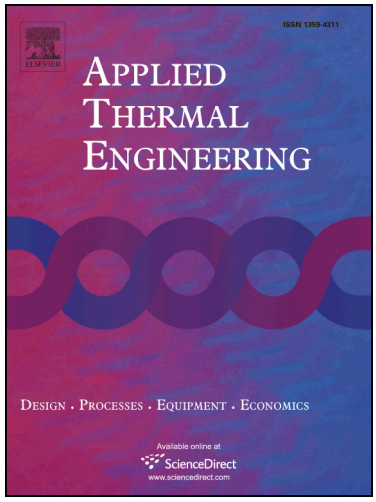

Exergetic, Economic, and Environmental Evaluations and Multi-objective Optimization of an Internal-Reforming SOFC-Gas Turbine Cycle Coupled with a Rankine Cycle

Mehdi Aminyavari, Alireza Haghighat Mamaghani, Ali Shirazi, Behzad Najafi, Fabio Rinaldi

PII: S1359-4311(16)31324-2
DOI: http://dx.doi.org/10.1016/j.applthermaleng.2016.07.180
Reference: ATE 8778

To appear in: *Applied Thermal Engineering*

Received Date: 22 May 2016
Revised Date: 6 July 2016
Accepted Date: 28 July 2016

Please cite this article as: M. Aminyavari, A.H. Mamaghani, A. Shirazi, B. Najafi, F. Rinaldi, Exergetic, Economic, and Environmental Evaluations and Multi-objective Optimization of an Internal-Reforming SOFC-Gas Turbine Cycle Coupled with a Rankine Cycle, *Applied Thermal Engineering* (2016), doi: http://dx.doi.org/10.1016/j.applthermaleng.2016.07.180

Exergetic, Economic, and Environmental Evaluations and Multi-objective Optimization of an Internal-Reforming SOFC-Gas Turbine Cycle Coupled with a Rankine Cycle

Mehdi Aminyavari[a], Alireza Haghighat Mamaghani[a], Ali Shirazi[b,*], Behzad Najafi[a], Fabio Rinaldi[a]

[a] Dipartimento di Energia, Politecnico di Milano, Via Lambruschini 4, 20156, Milano, Italy

[b] School of Mechanical and Manufacturing Engineering, The University of New South Wales (UNSW), Kensington, New South Wales, 2052, Australia

Abstract

In the present study, a detailed thermodynamic model for an internal-reforming solid oxide fuel cell-gas turbine (SOFC-GT) hybrid system integrated with a Rankine (steam) cycle is developed, and exergetic, economic and environmental analyses have been carried out on the plant. Considering the exergetic efficiency and the total cost rate of the system as conflicting objectives, a multi-objective optimization of the system is conducted to determine the optimal design point of the plant. A set of optimal solutions (Pareto front) is achieved, each of which is a trade-off between the chosen objectives. Finally, TOPSIS (Technique for Order Preference by Similarity to an Ideal Solution) decision-making method is used to choose the final optimal design parameters. The results demonstrate that the final optimal design of the proposed plant leads to an exergetic efficiency of 65.11% and total cost rate of 0.13745 €/s. Furthermore, the optimization results reveal that the integration of the Rankine cycle with the SOFC-GT system has led to an 8.84% improvement in the total exergetic efficiency of the plant, producing additional 8439.2 MWh of electricity and avoiding ~ 5,900 metric tons of carbon dioxide emissions annually.

[*]Corresponding author
E-mail address: a.shirazi@unsw.edu.au

Keywords: solid oxide fuel cell; gas turbine; Rankine Cycle; exergy; economic; multi-objective optimization

Nomenclature

A: area (m^2)

c_f: fuel unit cost (US$ MJ^{-1})

c_p: specific heat at constant pressure (kJ kg^{-1} K^{-1})

CRF: capital recovery factor

$\dot{C}_{env}$: social cost of air pollution (€ s^{-1})

$\dot{C}_{tot}$: total cost rate (€ s^{-1})

E: open circuit voltage (V), Energy (kJ)

e: specific exergy (kJ kg^{-1})

$\dot{E}$: exergy flow rate (kW)

$\bar{e}$: specific exergy (kJ $kmol^{-1}$)

F: Faraday constant (96485 C mol^{-1})

$\bar{g}_f$: Gibbs free energy of formation (J mol^{-1})

h: specific enthalpy (kJ kg^{-1})

$\bar{h}$: specific enthalpy (kJ $kmol^{-1}$)

I: current (A)

i: current density (A m^{-2}), interest rate (%)

k: specific heat ratio

K_p: equilibrium constant

LHV: low heating value (kJ kg^{-1})

$\dot{m}$: mass flow rate (kg s^{-1})

N: operational hours in a year

n: system life time (year)

$\dot{n}$: molar flow rate (kmol s^{-1})

p: pressure (kpa, bar), payback period (year)

$\dot{Q}$: heat transfer rate (kW)

$\bar{R}$: universal gas constant (kJ $kmol^{-1}$ K^{-1})

r_p: pressure ratio

s: specific entropy (kJ kg^{-1} K^{-1})

$\bar{s}$: molar specific entropy (kJ $kmol^{-1}$ K^{-1})

S/C: steam to carbon ratio

SMR: steam-methane reforming

T: temperature (K)

TIT: turbine inlet temperature (K)

U: overall heat transfer coefficient (kW m^{-2} K^{-1})

U_a: air utilization factor

U_f: fuel utilization factor

V: voltage (V)

$\dot{W}$: mechanical work (kW)

WGS: water-gas shift

x: molar fraction

Z: capital cost (US$)

$\dot{Z}$: capital cost rate (€ s^{-1})

Greek symbols

ε: effectiveness

η: efficiency

ρ: density (kg m^{-3})

Φ: maintenance factor

ψ: exergy efficiency

Superscripts

Q: heat transfer

W: work

PH: physical

CH: chemical

Subscripts

0: reference

a: anode

AC: air compressor

act: activation

ap: approach point

C: compressor

c: cold

CC: combustion chamber

conc: concentration

COND: condenser

cv: control volume

D: destruction

DC: direct current

ECO: economizer

elec: electrical

env: environment

EVA: evaporator

f: fuel

FC: fuel compressor

g: gas

GT: gas turbine

h: hot

i: inlet

is: isentropic

LMTD: logarithmic mean temperature difference

o: outlet

ohm: ohmic

PH: pre-heater

pp: pitch point

r: reforming

REC: recuperator

s: shifting, stream

SH: supper heater

ST: steam turbine

tot: total

w: water

1. Introduction

Due to the growing global energy consumption, inevitable depletion of fossil fuels, and increasing environmental concerns, more energy-efficient designs for power production have been investigated in the recent years [1-3]. Combined cycle power plants (CCPPs) have become attractive alternatives in power markets due to their higher overall thermal efficiency in comparison with independent Brayton or Rankine cycle [4-6]. Fuel cells are envisaged as promising candidates for next generation power sources because of their high-thermal efficiencies and significantly low emission levels. In conventional power generation systems, fuel oxidation takes place to generate heat which is then converted to electrical energy by means of gas turbines. On the other hand, fuel cells convert the fuel's chemical energy directly into electricity, while their efficiency is not subject to the limitation of Carnot efficiency [7]. As a result, they evade many of the limitations of combustion engines, offering more energetically

efficient fuel to power conversion [8, 9]. For decentralized electricity production, high-temperature fuel cells such as the molten carbonate fuel cell (MCFC) and the solid oxide fuel cell (SOFC) have received increasing attention [10]. Among various fuel cells, SOFC technology is very promising because of high-temperature exhaust gas exiting the fuel cell (between 600 °C and 1000 °C) which can be utilized for cogeneration or bottoming cycles purposes [11]. Synergetic effect of such systems leads to very high electrical efficiencies (above 60%) [12]. On one hand, the high rate of electrochemical reactions at high temperatures eliminates the necessity for expensive noble metal catalyst and, on the other hand, the possibility of direct reforming of fuel in the SOFC provides wider range of fuel candidates [13, 14]. Several mathematical models have been proposed to study heat and mass transfer and electrochemical reactions effects in SOFCs [15, 16]. The model proposed by Achenbach [17], which utilized differential and finite equations, provides an accurate three-dimensional and time-dependent approach for planar solid oxide fuel cell simulation. Mathematical modeling compared to experimental investigations is an economical and efficient tool to predict the SOFC performance and achieve design optimization. Several theoretical studies have been carried out on SOFC systems integrated with gas turbine cycles [18] as wells as their partial load performance [19, 20]. Akkaya and Sahin [21] developed a steady-state mathematical model of a combined SOFC and organic Rankine cycle and analyzed the plant performance from energetic standpoint. The results revealed that an integrated organic Rankine cycle (ORC) can improve the energy efficiency of the SOFC system up to 25%. Yan et al. [22] studied a system that integrates SOFC-GT with an ORC system which used liquefied natural gas (LNG) as heat sink to recover the cryogenic energy of LNG. Their result indicated that an overall electric efficiency of 67% could be achieved. The overall efficiency of a power generation system can be improved by recovering waste heat from the exhausts gas exiting the

gas turbine. This is achieved by directing the gas stream through heat exchangers and generating steam in a heat recovery steam generator (HRSG), which, in effect, is a heat exchanger that recovers heat from a hot gas stream and produces steam that can be utilized to drive a steam turbine. Different types of HRSGs are employed in industry and a conventional way to classify them is based on the number of pressure levels of the system − low pressure (LP), intermediate pressure (IP) and high pressure (HP). Main components of an HRSG can be narrowed down into an economizer, an evaporator and a superheater [23]. Considering only the efficiency of the gas turbine, gas turbine exhaust temperature should be minimized as much as possible, but this deteriorates the performance of the HRSG system. Therefore, one may consider a trade-off in choosing the exhaust gas temperature entering the bottoming cycle, even though it is commonly recommended that the system should operate at the maximum gas turbine efficiency. Sanjay [24] examined the effect of HRSG configuration on exergy destruction of the bottoming cycle components and found that the highest energy efficiency in the bottoming cycle can be seen in case of triple pressure reheat configuration. In another study [25], energy evaluation of the system revealed that heat losses at the HRSG decreases as the number of pressure levels of steam generation increases.

While hybrid SOFC–GT plants have been extensively studied by many researchers [26-28], very limited number of studies on feasibility of integrating solid oxide fuel cells and HRSG unit have been conducted. Previous investigations based on the first law of thermodynamics have shown that, due to the synergistic effects, the efficiency of an SOFC system integrated with a gas turbine and an HRSG unit can be as high as 70% [29]. Bavarsad [30] used an HRSG to recover the waste heat from an SOFC-gas turbine cycle, aiming at improving the energy efficiency of the whole plant. The results showed that the exergetic efficiency of the system can be enhanced up

to 70%. In a similar study, Motahar and Alemrajabi [31] suggested that utilizing an HRSG unit and injecting the steam into the cycle can boost the exergetic efficiency by 18%. Although the first law of thermodynamics is a useful tool in the analysis of thermal systems, it treats all forms of energy as equivalent and does not take into account their quality. In recent years, exergetic analysis, based on the first and second laws of thermodynamics, has been employed by many researches to gain new insights into quality of different forms of energy and determine the location, types and magnitude of losses [32].

In order to perform a comprehensive assessment of a new power generation plant, the economic aspects of the system should also be taken into account [33]. Several studies have been carried out on the economic and exergo-economic aspects of energy systems in order to provide a comprehensive understanding of their feasibility [34-36]. Cheddie [37] performed a thermo-economic optimization on a hybrid plant including an SOFC indirectly coupled with a 10 MW gas turbine system. The whole plant had an output of 18.9 MW and 48.5% thermal efficiency at optimum design point. Calise et al. [38] modeled and evaluated a hybrid SOFC-GT system from energetic, exergetic and economic aspects and conducted a single level thermo-economic optimization analysis on the system [39]. Sahoo [40] carried out the exergo-economic analysis and optimization of a cogeneration system and found that the electricity and production costs for the optimum case are almost 10% lower as compared to the base case.

In recent years, due to the increasing environmental concerns, a particular attention has been paid to the emission effects of power plants. Therefore, several studies [41, 42] have been conducted by considering the environmental impacts of these systems. Sayyaadi [41] performed a multi-objective exergo-economic and environmental optimization of a benchmark cogeneration plant. The results showed that the optimization process has led to 4.28% reduction in the environmental

cost impact and 7.17% reduction in the cost rate of the system product compared to the base case design. Suresh et al.[42] performed a 3E (energetic, exergetic and environmental) analysis of advanced power plants based on high ash coal and estimated the emissions of CO and particulates to study the environmental impact of the plants. The results showed that the maximum possible energy efficiency of the plant was about 42.3%.

Multi-objective optimization method is an efficient tool to optimize problems with conflicting objectives. Autissier et al. [43] performed a multi-objective thermo-economic optimization of an SOFC-GT hybrid system in order to maximize the electrical efficiency and minimize the investment cost of the system. They found that the electrical efficiency of 40- 70% can be achieved, while the cost of the system can vary between 2400 $/kW and 6700 $/kW. A similar study was carried out on a planar SOFC system for stationary applications by Palazzi et al. [44]. Recently, Sanaye et al.[45] conducted a multi-objective optimization on a SOFC system integrated with a micro gas turbine, where the exergetic efficiency and total cost of the system were considered as optimization objectives. Their optimization results suggested an optimal design leading to a total exergetic efficiency of 60.7%, with an electrical energy cost of 0.057 $\$kWh^{-1}$ and payback period of about 6.3 years for the investment.

To the best of the authors' knowledge, there has been no other study that encompasses a comprehensive investigation and optimization of an SOFC-GT coupled to a Rankine bottoming cycle unit from exergetic, economic, and environmental points of view. The present work builds on a previous study of the authors [28],where a thermo-economic-environmental model for an SOFC-GT hybrid power plant was investigated. An optimization procedure based on genetic algorithm has been applied to the whole system to obtain the optimum design parameters subject to a set of constraints. The considered objective functions are the exergetic efficiency (to be

maximized) and the total cost rate (to be minimized). The latter includes the capital and maintenance costs of system components, the operational cost, and the environmental penalty cost due to CO and NO emissions. Due to the conflicting nature of these two objectives, it is impossible to find a solution that simultaneously satisfies both of them. Therefore, the concept of Pareto optimal solution is utilized to determine optimal solutions. TOPSIS (technique for order preference by similarity to an ideal solution) decision making method is applied to choose the final optimum design point of the system.

2. System description

Fig. 1 indicates the schematic diagram of the considered combined SOFC-GT-ST system. The SOFC-GT cycle consists of an air compressor (AC), a fuel compressor (FC), an internal-reforming solid oxide fuel cell (IRSOFC) stack, a DC/AC inverter, an air recuperator (REC), a mixer, a combustion chamber (CC), gas turbines (GT), and an electric generator (~). The Rankine (stream) bottoming cycle is coupled with the gas cycle by means of a heat recovery steam generator (HRSG) and includes a steam turbine (ST), an electric generator (~), a condenser (Cond) and a feed water pump (Pump 1). The HRSG comprises a pre-heater (PH), a deaerator (DEA), a pump (Pump 2), a regenerator (REG), an economizer (ECO), an evaporator (EVA) and a superheater (SH).

As seen in Fig. 1, the ambient air at node 1 is compressed by the air compressor up to node 2, and is subsequently preheated in the air recuperator (REC) , reaching node 3. The compressed, preheated air enters the cathode compartment of the SOFC stack. Similarly, natural gas entering the plant at node 4 is pressurized by the fuel compressor up to the stack's operating pressure. Afterwards, the pressurized fuel passes through the mixer where it is mixed with the steam recirculated from the anode compartment. This is necessary for methane reforming and water gas

shifting. The resulting stream enters the anode compartment of the stack (node 6) where it undergoes the reforming process leading to hydrogen-rich products which participate in the electrochemical reaction taking place within the stack. The DC/AC inverter converts the DC power generated by the stack into grid quality electricity. The electrochemical reaction taking place inside the SOFC stack produces thermal energy which is divided into three parts. The first portion is used to provide the required heat of the internal reforming reaction, the second part is employed to heat up the cell products and residual reactants, and the remaining amount is transferred to the environment as a heat loss. The high temperature streams of air leaving the cathode side (node 7) and the exhausted fuel, the non-reacted part of the reformed natural gas, exiting the anode compartment (node 8) enter the combustion chamber where the remaining fuel as well as the auxiliary fuel is burnt with the excess air. The flue gas at node 10 goes through the gas turbine, where the necessary power to drive the fuel and air compressors is provided while the remaining mechanical power is converted to electrical energy by the generator. The flue gas expanded in the gas turbine (node 11) flows through the air recuperator and the remaining thermal energy left over at node 12 is utilized in the HRSG unit to produce superheated steam in order to drive the Rankine (steam) bottoming cycle. Eventually, the exhaust gas is discharged to the atmosphere at node 13.

In the Rankine cycle, water is pumped from node 14 to node 15 and enters the deaerator (node 16) after going through the preheating process. There is a continuous production of low-pressure steam which enters below the perforated trays in the deaerator and flows upward through the perforations. The hot deaerated water (node 17) flows down where it is pumped to the economizer (node 18). The high pressure nearly saturated water (node 19) as a consequence of economizer turns to saturated vapor in the evaporator (node 20). The resulting saturated vapor

then passes through the superheater, producing superheated steam (node 21) to run the steam turbine. The steam expansion through the steam turbine produces additional useful work which results in electrical power generation. Finally, the low-pressure steam exiting the turbine (node 22) enters the condenser, where it is condensed at a constant pressure and turns to saturated liquid water (node 14).

3. System analysis

In this section, a mathematical model of the proposed SOFC-GT-ST system based on thermal (energetic and exergetic), economic, and environmental analyses is presented.

3.1. Energetic analysis

Based on the first law of thermodynamics, a thermodynamic model of the whole plant is presented in this section. The following assumptions have been considered to simplify the modeling of the system:

- All gases are treated as ideal gases[46].
- All chemical reactions are in equilibrium[28].
- Internal distribution of temperature, pressure, and gas compositions in each component is uniform [47, 48].
- Cathode and anode temperatures are assumed to be the same[49].
- The kinetic and potential energies of the fluid streams are negligible [10, 28, 50].
- All system components, except for fuel cell stack and combustion chamber, are adiabatic [28, 51].
- All system components operate under steady-state conditions[52].
- Gas/steam leakage is negligible [46].

3.1.1. Compressor

The isentropic efficiency of the compressor (η_c) is defined as follows:

$$\eta_C = \frac{h_{o,is} - h_i}{h_o - h_i} \quad (1)$$

This equation is used to determine the working fluid temperature at the compressor outlet. The compressor power consumption ($\dot{W}_C$) is obtained as:

$$\dot{W}_C = \dot{m}\left(h_o - h_i\right) \quad (2)$$

It should be mentioned that aforementioned relations can also be used for both air and fuel compressors.

3.1.2. SOFC stack

A tubular design SOFC model has been developed in the present work and the geometric and performance related data are according to Ref. [53]. In an SOFC unit, DC power is generated via electrochemical reactions. The hydrogen produced as a result of natural gas reforming inside the anode compartment is oxidized in the stack. The basic electrochemical reactions simultaneously occurring inside the SOFC stack are given as follows:

$$CH_4 + H_2O \rightarrow CO + 3H_2 \quad \text{(SMR reaction)} \quad (3)$$

$$CO + H_2O \rightarrow CO_2 + H_2 \quad \text{(WGS reaction)} \quad (4)$$

$$H_2 + \frac{1}{2}O_2 \rightarrow H_2O \quad \text{(Electrochemical)} \quad (5)$$

Therefore, the net chemical reaction inside the cell can be written as:

$$CH_4 + 2O_2 \rightarrow CO_2 + 2H_2O \quad (6)$$

The equilibrium constants for reforming and shifting reactions as a function of partial pressures can be obtained as follows:

$$K_{p,r} = \frac{p_{CO} p_{H_2}^3}{p_{CH_4} p_{H_2O}} \tag{7}$$

$$K_{p,s} = \frac{p_{CO_2} p_{H_2}}{p_{CO} p_{H_2O}} \tag{8}$$

The equilibrium constants can also be defined by the following temperature-dependent equation:

$$\mathrm{Log}\left(K_p\right) = AT^4 + BT^3 + CT^2 + DT + E \tag{9}$$

where the constant values for both reforming and shifting reactions can be found in [30].

Assuming x, y, and z are the molar flow rate of CH_4, CO, and H_2 participating in the chemical reactions inside the stack, one can write:

$$K_{p,r} = \frac{\left[\frac{\left(\dot{n}_{CO,i} + x - y\right)}{\dot{n}_{tot,i} + 2x}\right] \times \left[\frac{\left(\dot{n}_{H_2,i} + 3x + y - z\right)}{\dot{n}_{tot,i} + 2x}\right]^3}{\left[\frac{\left(\dot{n}_{CH_4,i} - x\right)}{\dot{n}_{tot,i} + 2x}\right] \times \left[\frac{\left(\dot{n}_{H_2O,i} - x - y + z\right)}{\dot{n}_{tot,i} + 2x}\right]} \times \left(\frac{p_{SOFC}}{p_0}\right)^2 \tag{10}$$

$$K_{p,s} = \frac{\left[\frac{\left(\dot{n}_{CO_2,i} + y\right)}{\dot{n}_{tot,i} + 2x}\right] \times \left[\frac{\left(\dot{n}_{H_2,i} + 3x + y - z\right)}{\dot{n}_{tot,i} + 2x}\right]}{\left[\frac{\left(\dot{n}_{CO,i} + x - y\right)}{\dot{n}_{tot,i} + 2x}\right] \times \left[\frac{\left(\dot{n}_{H_2O,i} - x - y + z\right)}{\dot{n}_{tot,i} + 2x}\right]} \tag{11}$$

$$z = U_f\left(3x + y\right) \tag{12}$$

where $\dot{n}_{tot,i}$ and U_f are the total inlet molar flow rate and the fuel utilization factor, respectively.

Knowing the stack temperature, the equilibrium constants can be computed from Eq.(9), and the unknowns x, y, and z are determined throughout solving Eqs. (10)-(12) Simultaneously. The stack DC current (I) can be calculated as follows:

$$I = 2Fz = iA_{SOFC} \tag{13}$$

The open circuit reversible cell voltage (E) can be obtained from Nernst equation as [35]:

$$E = \frac{-\Delta \bar{g}_f^0}{2F} + \frac{\bar{R}T}{2F} \ln\left(\frac{p_{H_2} p_{O_2}^{\frac{1}{2}}}{p_{H_2O}} \right) \tag{14}$$

where $\Delta \bar{g}_f^0$ is the change in molar Gibbs free energy of formation at standard pressure, and T is the stack temperature. As a consequence of several types of irreversible losses in a real cell, the actual operating voltage of SOFC is less than the reversible one. Thus, the cell actual voltage (V_{cell}) can be declared as:

$$V_{cell} = E - \Delta V_{loss} \tag{15}$$

where ΔV_{loss} is the sum of voltage losses subsume of activation overvoltage (V_{act}), ohmic overvoltage (V_{ohm}), and concentration overvoltage (V_{conc}). These losses can be determined through comprehensive empirical relations available in literature [7, 13, 29, 53].The DC electrical power generated by the stack ($\dot{W}_{SOFC,DC}$) can determined by:

$$\dot{W}_{SOFC,DC} = V_{cell} I \times 10^{-3} = V_{cell} iA_{SOFC} \times 10^{-3} \tag{16}$$

The calculation procedures for determining the thermal energy generated within the SOFC stack and subsequently the stack temperature were explained in detail in the previous work of the authors [28].

3.1.3. Combustion chamber

The flue gas stream leaving the combustion chamber primarily supplies the required energy to drive the gas turbine and the HRSG for further electricity production. The gas temperature at the combustion chamber outlet can be calculated by applying the first law of thermodynamics to the combustion chamber:

$$-\dot{Q}_{loss,CC} + \sum_{R} \dot{n}_i \bar{h}_i - \sum_{P} \dot{n}_o \bar{h}_o = 0 \quad (17)$$

where

$$\dot{Q}_{l,CC} = \dot{m}_f \left(1 - U_f\right) \times \left(1 - \eta_{CC}\right) \times LHV_f \quad (18)$$

Eq. (17) is used to modify the gas turbine inlet temperature (which is guessed initially) until the convergence criterion is met [28].

3.1.4. Gas turbine

The mechanical work produced in the gas turbines ($\dot{W}_{GT}$) can be determined as follows:

$$\dot{W}_{GT} = \dot{m}_{10} \left(h_{10} - h_{11}\right) \quad (19)$$

As illustrated in Fig. 1, the gas turbine provides the power requirement of the air and fuel compressors and transfers the remaining mechanical power to the generator for electricity generation.

3.1.5. Recuperator

The effectiveness of the recuperator (ε) is defined as follows [8]:

$$\varepsilon = \frac{T_{h,i} - T_{h,o}}{T_{h,i} - T_{c,i}}, \quad \text{if:} C_h < C_c \quad (20)$$

$$\varepsilon = \frac{T_{c,o} - T_{c,i}}{T_{h,i} - T_{c,i}}, \quad \text{if:} C_c < C_h \quad (21)$$

where $T_{c,i}$ and $T_{c,o}$ are the inlet and outlet temperatures of the cold fluid, $T_{h,i}$ and $T_{h,o}$ are the inlet and outlet temperatures of the hot fluid, and finally C_c and C_h are the heat capacity rate of the cold and hot fluids, respectively. The energy balance equation of the recuperator and the correlation for calculating the corresponding surface can be found in the authors' previous work [28].

3.1.6. Mixer

The mixer is employed to mix the steam recirculation from the anode compartment with the compressed fuel, providing the required steam-to-carbon ratio to perform the fuel reforming reaction. Mass and energy balance equations are used to model this component as follows:

$$\dot{m}_5 + \dot{m}_9 = \dot{m}_6 \tag{22}$$

$$\dot{m}_5 h_5 + \dot{m}_9 h_9 = \dot{m}_6 h_6 \tag{23}$$

3.1.7. Water pump

The water pump power consumption ($\dot{W}_{pump}$) can be determined by [8]:

$$\dot{W}_{pump} = \frac{\dot{m}_w \times \Delta p_{pump}}{\rho_w \times \eta_{pump}} \tag{24}$$

where $\dot{m}_w$, Δp_{pump}, and η_{pump} are the mass flow rate of water, water pressure rise through the pump, and the pump isentropic efficiency, respectively.

3.1.8. HRSG

The heat recovery steam generator (HRSG) is required to integrate the SOFC-GT cycle with the steam cycle. In other words, this component is used to recover the remaining thermal energy of the high temperature exhaust gases at node 12 and to provide the required steam to drive the

steam turbine. Three important design parameters of an HRSG unit are the pinch point and the approach point, which govern the gas temperature profile, along with the evaporation pressure. The approach point can be defined as the temperature difference between superheated steam leaving the superheater (T_{21}) and the gas temperature entering the HRSG (T_{12}):

$$\Delta T_{ap} = T_{12} - T_{21} \tag{25}$$

The pinch point represents the minimum difference between the gas temperature leaving the evaporator and the steam saturation temperature which can be obtained as follows:

$$\Delta T_{pp} = T_{12b} - T_{20} \tag{26}$$

Another design parameter that should be taken into account is called sub-cooled temperature difference which can be presented as follow:

$$\Delta T_{pp} = T_{20} - T_{19} \tag{27}$$

The energy balance equation for the pre-heater, economizer, evaporator, and superheater can be expressed as follows[54]:

$$\dot{Q}_{PH} = \dot{m}_g \left(h_{12d} - h_{13}\right) = \dot{m}_s \left(h_{16} - h_{15}\right) \tag{28}$$

$$\dot{Q}_{ECO} = \dot{m}_g \left(h_{12b} - h_{12c}\right) = \dot{m}_s \left(h_{19} - h_{18}\right) \tag{29}$$

$$\dot{Q}_{EVA} = \dot{m}_g \left(h_{12a} - h_{12b}\right) = \dot{m}_s \left(h_{20} - h_{19}\right) \tag{30}$$

$$\dot{Q}_{SH} = \dot{m}_g \left(h_{12} - h_{12a}\right) = \dot{m}_s \left(h_{21} - h_{20}\right) \tag{31}$$

3.1.9. Steam turbine and condenser

The mechanical work generated through the steam turbine can be determined as follows:

$$\dot{W}_{ST} = \dot{m}_s \left(h_{21} - h_{22}\right) \tag{32}$$

The isentropic efficiency of the steam turbine (η_{ST}) can be written as follows:

$$\eta_{ST} = \frac{h_{21} - h_{22}}{h_{21} - h_{22,is}} \tag{33}$$

The downstream pressure at the steam turbine is obtained by:

$$p_{22} = p_{21}\left(\frac{T_{22,is}}{T_{21}}\right)^{\frac{k_s}{k_s - 1}} \tag{34}$$

The heat transfer rate at the condenser can determined as follows:

$$\dot{Q}_{COND} = \dot{m}_s \left(h_{22} - h_{14}\right) \tag{35}$$

3.1.10. Energetic efficiency

The energetic (electrical) efficiency of the plant can be defined as follows:

$$\eta_{elec} = \frac{\dot{W}_{net,elec}}{\dot{m}_f \times LHV_f} \tag{36}$$

where

$$\dot{W}_{net,elec} = \dot{W}_{SOFC,AC} + \dot{W}_{ST,elec} + \dot{W}_{GT,elec} - \dot{W}_{AC,elec} - \dot{W}_{FC,elec} - \dot{W}_{pumps,elec} \tag{37}$$

The equations for calculating the work transfer rates of the SOFC, gas turbine , compressors and pumps can be found in the previous work of the authors [28].

The work transfer rate of the steam turbine can be determined by:

$$\dot{W}_{ST,elec} = \eta_{elec,ST} \times \dot{W}_{ST} \tag{38}$$

3.2. Exergetic analysis

Exergy is defined as the maximum work gained from a system when it reaches equilibrium with the surrounding environment from its initial state. The exergetic analysis based on the second law of thermodynamics allows one to identify the location of losses and thermodynamic

irreversibilities in a thermal system [55]. The steady state form of exergy balance equation for a control volume can be expressed as follows:

$$\frac{dE_{CV}}{dt} = \sum_j \dot{E}_j^Q - \dot{E}^W + \sum_i \dot{E}_i - \sum_o \dot{E}_o - \dot{E}_D = 0 \quad (39)$$

where $\dot{E}^Q$ and $\dot{E}^W$ are the rate of exergy associated with heat and work transfers respectively, $\dot{E}_i$ and $\dot{E}_e$ are the exergy transfer rate at control volume inlets and outlets, and $\dot{E}_D$ is the exergy destruction rate due to thermodynamic irreversibilities. In absence of electromagnetic, electric, nuclear, and surface tension effects and assuming the change in potential and kinetic energies negligible, the exergy flow rate of the system is divided into two parts − physical and chemical exergy [22, 55]:

$$\dot{E} = \dot{E}^{PH} + \dot{E}^{CH} \quad (40)$$

The physical exergy can be determined by:

$$\dot{E}^{PH} = \dot{m}\left[\left(h - h_0\right) - T_0\left(s - s_0\right)\right] \quad (41)$$

The chemical exergy of gaseous mixtures can be calculated by:

$$\dot{E}^{CH} = \dot{n}\left[\sum_K X_K \bar{e}^{CH} + \bar{R}T_0 \sum_K X_K \ln X_K\right] \quad (42)$$

Using Eq. (39), the exergy destruction rate for each system component is summarized in Table 1.It should be noted that the exergy destruction of Pump 2 has been included within the exergy destruction of the HRSG unit.

3.3. Economic analysis

In order to comprehensively analyze the performance of a power plant, the economic aspects of the system should also be taken into account as this determines whether or not it makes sense to

actually build such plants. Therefore, to investigate the economic performance of the proposed plant, a detailed economic model was developed in which the capital and maintenance costs of the system components as well as the operational cost of the plant (i.e. the cost associated with fuel consumption) have been taken into account. As part of this calculation, the nominal cost of CO_2 emissions released into the atmosphere was also added to the total cost rate of the plant. The following details the cost elements contributing to the total cost of the proposed system.

3.3.1. Capital, maintenance, and operational costs

The purchased equipment cost of each system component (Z_k) is estimated based on the cost functions listed in Table 2, which have been estimated based on the data provided by manufactures and the information available in the literature [7, 52, 56-61].The following equation is used to convert the capital cost to cost per unit of time ($\dot{Z}_k$):

$$\dot{Z}_k = \frac{Z_k \times CRF \times \Phi}{N \times 3600} \tag{43}$$

where Φ is the maintenance factor, N is the annual operational hours of the system, and CRF is the capital recovery factor which is obtained based on the considered interest rate (i) and life time of the system (n) [22]:

$$CRF = \frac{i(1+i)^n}{(1+i)^n - 1} \tag{44}$$

Furthermore, the cost rate corresponding to the fuel cost based on the unit cost of fuel (c_f) can be determined as:

$$\dot{C}_f = c_f \times \left(\frac{LHV}{1000} \right) \times \dot{m}_f \tag{45}$$

where c_f is the unit cost of fuel.

3.4. Environmental analysis

Global warming and environmental issues have become a widespread concern in the recent years, which necessitates considering the environmental impacts of energy systems in design process [55, 62]. Accordingly, in the present work, the CO, NO_x and CO_2 emissions are considered as important factors and their equivalent social costs are summed up with the total cost rate of the cycle. Data reported from several experiments indicate that the amount of carbon monoxide and nitrogen oxides emissions produced within the SOFC stack is negligible [63]. The amounts of CO and NO_x production within the combustion chamber, based on the residence time in the combustion zone (τ) and the primary zone combustion temperature (T_{pz}) can be determined by [64]:

$$m_{CO} = \frac{0.179\times10^{9}\times\exp\left(\frac{7800}{T_{pz}}\right)}{p^{2}\tau\left(\frac{\Delta p}{p}\right)^{0.5}} \tag{46}$$

$$m_{NO_x} = \frac{0.15\times10^{16}\times\tau^{0.5}\exp\left(\frac{-71100}{T_{pz}}\right)}{p^{0.05}\left(\frac{\Delta p}{p}\right)^{0.5}} \tag{47}$$

where $\frac{\Delta p}{p}$ indicates the non-dimensional pressure drop in the combustion chamber. Detailed relations for determining τ and T_{pz} are given in Refs. [61, 64]. It should be mentioned that the amount of CO_2 emission into the atmosphere is determined based on combustion equation in the combustion chamber.

4. System optimization

4.1. Definition of the objective functions

In the present work, the exergetic efficiency(48) and the total cost rate of the plant are considered as the objective functions used for the multi-objective optimization procedure. The mentioned objective functions can be expressed using the following relations:

Exergeticefficiency (objective function I)

$$\psi_{tot} = \frac{\dot{E}_{out}}{\dot{E}_{in}} = \frac{\left(\dot{W}_{SOFC,AC} + \dot{W}_{ST} + \dot{W}_{GT} - \dot{W}_{AC} - \dot{W}_{FC} - \dot{W}_{pumps}\right)}{\dot{m}_f e_f^{CH}} = 1 - \left(\frac{\dot{E}_{D,tot}}{\dot{m}_f e_f^{CH}}\right) \quad (48)$$

where $\dot{E}_{D,tot}$ is the sum of exergy destruction rate of all system components, and e_f^{CH} denotes the specific chemical exergy of the fuel (natural gas).

Total cost rate (objective function II)

$$\dot{C}_{tot} = \sum_k \dot{Z}_k + \dot{C}_f + \dot{C}_{env} \quad (49)$$

where

$$\dot{C}_{env} = c_{CO}\dot{m}_{CO} + c_{NO_x}\dot{m}_{NO_x} + c_{CO_2}\dot{m}_{CO_2} \quad (50)$$

$\dot{m}_{NO_x}$, $\dot{m}_{CO}$, and $\dot{m}_{CO_2}$ are the exhaust mass flow rates of nitrogen oxides, carbon monoxide, and carbon dioxide respectively, while c_{NO_x}, c_{CO}, and c_{CO_2} are their corresponding damage unit costs.

4.2. Design parameters and constraints

The following design parameters are chosen for optimization of the system: the air compressor pressure ratio ($r_{p,AC}$),current density (i), utilization factor of air (U_a) and fuel (U_f), steam to

carbon ratio (S/C) and the HRSG evaporation pressure (P_{eva}).The foregoing design parameters and their range of variation as well as the system constraints are listed in Table 3.

4.3. Genetic algorithm and multi-objective optimization

Genetic algorithm is a promising technique for solving the multi-objective optimization problems[65, 66]. In the flowchart presented in Fig. 2, various stages of GAs optimization process have been illustrated .New generations of solutions are produced from the previous ones by means of crossover and mutation operators. As the search goes on, the population converges, and at last is dominated by a set of solutions. Once a set of solutions, called a Pareto optimal set, is achieved, the decision-maker decides which optimal design point is suitable for the specific considered project [67].

5. Case study

The SOFC-GT-ST combined cycle modeled in the present work is considered to be installed in Milan, Italy. An HRSG unit is utilized to produce the required steam for the Rankine cycle via recovering the extra heat of the flue gas. The input parameters listed in Table 4 and 5 are taken into consideration for simulation of the system. It should be noted that the atmospheric conditions were considered as the dead state in the exergetic analysis of the plant. Thus, T_0 and P_0 were assumed to be equal to 25 °C and 1 atm, respectively. Moreover, the thermodynamic properties of each stream of the plant at the base operating condition ($r_{p,\,AC=}8$;i=4500 A/m^2; U_a=0.35; U_f=0.75; S/C=3; P_{eva}=20) are reported in Table 6. The fuel unit cost (c_f) is considered to be 0.4 €/m^3[65]. In addition, the unit damage cost related with $CO\left(c_{CO}\right)$, $NO_x\left(c_{NO_x}\right)$ and $CO_2\left(c_{CO_2}\right)$ are considered to be 0.01642 €/kg CO, 5.396 €/kg NO_x and 0.0176 €/kg CO_2, respectively [28, 68]. The approximate lifetime of the system (n), the annual operational hours

(N), the maintenance factor (Φ), and the annual interest rate (i) are considered to be 15 years, 8000 hours, 1.06, and 1.7 % [69], respectively.

6. Results and discussion

6.1. Model verification

Details about verification of the SOFC–GT hybrid cycle were presented in detail in the previous work of the authors [28]. Since the SOFC stack is a critical component of the system, the authors preferred to also validate its behavior separately; therefore a comparison has also been drawn on the current density–voltage curve generated by the present model and the one reported by Chan et al. [29]. In order to have an accurate comparison, the working temperature and pressure have been set to be the same as the ones considered in the case study presented in Ref. [29]. As demonstrated in Fig. 3, it can be seen that the present simulation results are in agreement with the reported data in Ref. [29] with a margin of 5%, which verifies sufficient accuracy of the developed model to simulate the thermal performance of the SOFC system. Details on verification of the gas turbine and steam turbine can be found in the previous works of the authors [10, 68].

6.2. Optimization results

As shown in Table 3, in the present study, six design parameters have been taken into account in order to maximize the exergetic efficiency and minimize the total cost rate of the plant. The tuning parameters for the genetic algorithm procedure employed for the system optimization are as follows: population size: 120, crossover probability: 0.8, and gene mutation probability: 0. 01. A tolerance of 10^{-4} was set as the stopping criteria, ensuring that the weighted average change in

the fitness function value over stall generations is small enough before the algorithm terminates the optimization process.

Fig. 4 demonstrates the Pareto optimal solutions achieved from multi-objective optimization of the system. The trend of the Pareto front evidently shows the conflicting nature of the considered objectives. As can be seen in this figure, increasing the exergetic efficiency up to about 60% does not significantly increase the total cost rate of the system, while increasing it from 60% to 65% results in a moderate increase in the total cost rate of the system. Increasing the exergetic efficiency beyond 65%, leads to a steep rise in the total cost rate of the plant. This is because as the exergetic efficiency exceeds 65%, the optimal decision variables shift to a more thermodynamically efficient design, resulting in a dramatic increase in the capital costs of the system components. Thus, optimizing the system by only considering the exergetic efficiency as the objective function would lead to the selection of design point A (Case A) where the highest exergetic efficiency (67.18%) and the highest total cost rate of the system (0.1847 €/s) are achieved. On the other hand, design point B (Case B) would be the optimal solution if the total cost rate of the system was selected as the only objective function. This leads to the minimum value of the total cost rate (0.1271€/s) and the lowest exergetic efficiency of the system (41.71%).In other words, Case A represents the situation where the thermodynamic objective (exergetic efficiency) is most weighted, while Case B has been mostly weighted in favor of economic objective (total cost rate of the system). In multi-objective optimization, each solution on the Pareto front can be considered as an optimal point; therefore, selection of the final optimum solution depends on preferences and criteria of each decision-maker (e.g. efficiency and economic criteria).In the present work, after Euclidian non-dimensionalization of all objectives, TOPSIS (Technique for Order Preference by Similarity to an Ideal Solution) method

has been used to specify the final optimum design point of the system. In this method, one should first define the ideal and non-ideal points. The ideal point is the point at which the optimum value of one objective is obtained separately, without fulfilling other objective. The non-ideal point, on the other hand, is defined as the point at which the worst value for each objective is obtained. TOPSIS method indicates that the final optimal point must be in the shortest possible distance from the ideal point and the farthest distance from the non-ideal one [70, 71]. Consequently, both the distance from the ideal point (d^+) and the non-ideal point (d^-) should be calculated for all of the optimal solution points and the solution with the maximum value of a closeness coefficient, defined as $\frac{d^-}{d^- + d^+}$, should be selected as the final optimal point, which is marked in Fig. 5. This point corresponds to an exergetic efficiency of 65.11% and the total cost rate of 0.13745 €/s. The optimal design parameters of the system for Case A and B as the two design extremes as well as the final optimal design point from the TOPSIS decision-making method are listed in Table 7. As mentioned before, one of the main purposes of the present study is to evaluate the economic viability of the proposed system and also to underline the significance of using multi-objective optimization in finding the best trade-off between the economic indexes and thermodynamic performance of the system. In order to demonstrate the locations where the exergy losses occur, the exergy destruction rate of each component is given in Fig. 6. These values are obtained at different optimal points achieved by the three foregoing optimization standpoints. The practical utility of performing the exergetic analysis is in determining the location and true magnitude of exergy waste due to thermodynamic irreversibilities and inefficiencies. Such information can be useful to show the room for improvement and to identify specific components which limit the system. As demonstrated in Fig. 6, the highest exergy destruction rate takes place in the SOFC stack and the combustion

chamber. Thus, this study indicates that these components warrant substantial future research and development (in terms of fluid mechanics, materials science, and heat transfer) to improve their design and performance to achieve fully optimized integrated SOFC-GT-ST systems. The next highest exergy destruction rates take place at the HRSG unit, the steam turbine, and the condenser. The required capital costs of the system components at the different optimal design points are shown in Table 8.The main share of the capital cost is accounted for the SOFC stack, varying from 40% to 55% of the total capital cost of the plant. Furthermore, the next highest capital cost is associated with the gas turbine, steam turbine, and the HRSG unit. As seen in Table 8, the total cost rate of the final optimum point selected by TOPSIS lies between that of the two extremes (Case A and B).

Furthermore, the results related to the performance of the proposed system at the aforementioned optimal points are presented in Table 9. As seen in this table, the plant design at point A, where the exergetic efficiency is the most weighted objective, leads to the most thermodynamically efficient design, resulting in a significant increase in the total cost rate of the system. Although the gain in the exergetic efficiency at Case A is not significant compared to that of the final optimal point, it is dramatically costly to design the plant based on this point (only 2.07% efficiency enhancement at the cost of 1.36 M€). By employing the multi-objective procedure, however, a trade-off between the thermodynamic efficiency and the cost of the system is obtained, which results in an exergetic efficiency of 65.11% and a total cost rate of 0.13745 €/s. According to Table 9, the power outputs from the SOFC, gas turbine and the steam turbine at the final optimal design point of the plant are 5.282 MW, 3.358 MW, and 1.055 MW respectively, which leads to the net electricity output of 7.761 MW from the proposed combined system. Finally, Fig. 7 shows the amount of both annual power output enhancement and CO_2 emissions

reduction of the proposed plant for Case A and B as well as the final optimal design point from the TOPSIS decision-maker as compared to a system without a bottoming cycle to recover the waste heat from the exhausts gas exiting the gas turbine. It should be noted that the amount of carbon dioxide emissions reduction has been determined based on an estimate of how much CO_2 would have been emitted by a conventional power plant to produce an equivalent amount of electricity produced by employing the bottoming cycle in the proposed combined plant. Finally, the multi-objective optimization results show that coupling the Rankine bottoming cycle with the main SOF-GT cycle has led to an 8.84% increase in the overall exergetic efficiency of the plant, yielding 8439.2 MWh/year additional electricity generation and avoiding about 5,900 metric tons of carbon dioxide emissions annually. Overall, the approach employed in this work, can be applied to similar high temperature fuel cell based power production units in order to enhance the overall efficiency of the system.

7. Conclusion

In the present study, an SOFC-GT plant integrated with a Rankine cycle was modeled and analyzed from energetic, exergetic, economic, and environmental perspectives. Multi-objective optimization of the system was performed, where the exergetic efficiency and total cost rate of the cogeneration system were considered as the objective functions. Beside the capital investment cost and operational costs, the environmental cost, representing the social costs of CO, NO_x and CO_2 emissions, was also taken into account to determine the total cost rate of the system. Considering the conflicting nature of the foregoing objectives, a set of optimal solutions was determined. Employing the TOPSIS decision-making method, the final optimal design point of the plant was selected. The results demonstrated that the most economical design of the plant leads to the minimum total cost rate of 0.127143 €/s and the lowest exergetic efficiency of

41.71%. On the other hand, the most energy-efficient design of the plant would be achieved if the thermodynamic objective (exergetic efficiency) was most weighted, reaching the exergetic efficiency of 67.18%; however, it results in the maximum total cost rate of 0.18469 €/s. Eventually, it was observed that the final design point selected by the TOPSIS method results in the best trade-off between the economic indexes and thermodynamic performance of the plant, achieving an exergetic efficiency of 65.11% and the total cost rate of 0.13745 €/s. Finally, it was found that coupling the Rankine bottoming cycle with the SOFC-GT plant has enhanced the overall exergetic efficiency of the system up to 8.84%, representing 8439.2 MWh/year additional electrical power production and avoiding about 5,900 metric tons of carbon dioxide emissions annually. Overall, the present work provides a theoretical groundwork for the energy-efficient and cost-effective design of high temperature fuel cell based combined power generation cycles.

References

[1] A.H. Mamaghani, S.A.A. Escandon, B. Najafi, A. Shirazi, F. Rinaldi, Techno-economic feasibility of photovoltaic, wind, diesel and hybrid electrification systems for off-grid rural electrification in Colombia, Renewable Energy, 97 (2016) 293-305.

[2] A. Bazyari, A.A. Khodadadi, A.H. Mamaghani, J. Beheshtian, L.T. Thompson, Y. Mortazavi, Microporous titania–silica nanocomposite catalyst-adsorbent for ultra-deep oxidative desulfurization, Applied Catalysis B: Environmental, 180 (2016) 65-77.

[3] A. Haghighat Mamaghani, S. Fatemi, M. Asgari, Investigation of influential parameters in deep oxidative desulfurization of dibenzothiophene with hydrogen peroxide and formic acid, International Journal of Chemical Engineering, 2013 (2013).

[4] A. Rovira, C. Sánchez, M. Muñoz, M. Valdés, M.D. Durán, Thermoeconomic optimisation of heat recovery steam generators of combined cycle gas turbine power plants considering off-design operation, Energy Conversion and Management, 52 (2011) 1840-1849.

[5] A.L. Polyzakis, C. Koroneos, G. Xydis, Optimum gas turbine cycle for combined cycle power plant, Energy Conversion and Management, 49 (2008) 551-563.

[6] M. Ghazi, P. Ahmadi, A.F. Sotoodeh, A. Taherkhani, Modeling and thermo-economic optimization of heat recovery heat exchangers using a multimodal genetic algorithm, Energy Conversion and Management, 58 (2012) 149-156.

[7] B. Najafi, A. Haghighat Mamaghani, A. Baricci, F. Rinaldi, A. Casalegno, Mathematical modelling and parametric study on a 30 kWel high temperature PEM fuel cell based residential micro cogeneration plant, International Journal of Hydrogen Energy, 40 (2015) 1569-1583.

[8] B. Najafi, A. Haghighat Mamaghani, F. Rinaldi, A. Casalegno, Long-term performance analysis of an HT-PEM fuel cell based micro-CHP system: Operational strategies, Applied Energy, 147 (2015) 582-592.

[9] B. Najafi, A.H. Mamaghani, F. Rinaldi, A. Casalegno, Fuel partialization and power/heat shifting strategies applied to a 30 kW el high temperature PEM fuel cell based residential micro cogeneration plant, International Journal of Hydrogen Energy, 40 (2015) 14224-14234.

[10] A. Haghighat Mamaghani, B. Najafi, A. Shirazi, F. Rinaldi, 4E analysis and multi-objective optimization of an integrated MCFC (molten carbonate fuel cell) and ORC (organic Rankine cycle) system, Energy, 82 (2015) 650-663.

[11] S.C. Singhal, K. Kendall, High-temperature Solid Oxide Fuel Cells: Fundamentals, Design, and Applicatons, Elsevier, 2003.

[12] L. Magistri, R. Bozzo, P. Costamagna, A.F. Massardo, Simplified Versus Detailed Solid Oxide Fuel Cell Reactor Models and Influence on the Simulation of the Design Point Performance of Hybrid Systems, Journal of Engineering for Gas Turbines and Power, 126 (2004) 516-523.

[13] M. Ni, D.Y.C. Leung, M.K.H. Leung, Electrochemical modeling and parametric study of methane fed solid oxide fuel cells, Energy Conversion and Management, 50 (2009) 268-278.

[14] A.H. Mamaghani, B. Najafi, A. Casalegno, F. Rinaldi, Long-term economic analysis and optimization of an HT-PEM fuel cell based micro combined heat and power plant, Applied Thermal Engineering, 99 (2016) 1201-1211.

[15] Y. Lu, L. Schaefer, P. Li, Numerical study of a flat-tube high power density solid oxide fuel cell: Part I. Heat/mass transfer and fluid flow, Journal of Power Sources, 140 (2005) 331-339.

[16] X. Xue, J. Tang, N. Sammes, Y. Du, Dynamic modeling of single tubular SOFC combining heat/mass transfer and electrochemical reaction effects, Journal of Power Sources, 142 (2005) 211-222.

[17] E. Achenbach, Three-dimensional and time-dependent simulation of a planar solid oxide fuel cell stack, Journal of Power Sources, 49 (1994) 333-348.

[18] S.H. Chan, H.K. Ho, Y. Tian, Modelling of simple hybrid solid oxide fuel cell and gas turbine power plant, Journal of Power Sources, 109 (2002) 111-120.

[19] S. Campanari, Full Load and Part-Load Performance Prediction for Integrated SOFC and Microturbine Systems, Journal of Engineering for Gas Turbines and Power, 122 (2000) 239-246.

[20] P. Costamagna, L. Magistri, A.F. Massardo, Design and part-load performance of a hybrid system based on a solid oxide fuel cell reactor and a micro gas turbine, Journal of Power Sources, 96 (2001) 352-368.

[21] A.V. Akkaya, B. Sahin, A study on performance of solid oxide fuel cell-organic Rankine cycle combined system, International Journal of Energy Research, 33 (2009) 553-564.

[22] Z. Yan, P. Zhao, J. Wang, Y. Dai, Thermodynamic analysis of an SOFC–GT–ORC integrated power system with liquefied natural gas as heat sink, International Journal of Hydrogen Energy, 38 (2013) 3352-3363.

[23] H. Hajabdollahi, P. Ahmadi, I. Dincer, An Exergy-Based Multi-Objective Optimization Of A Heat Recovery Steam Generator (HRSG) In A Combined Cycle Power Plant (CCPP) Using Evolutionary Algorithm, International Journal of Green Energy, 8 (2011) 44-64.

[24] Sanjay, Investigation of effect of variation of cycle parameters on thermodynamic performance of gas-steam combined cycle, Energy, 36 (2011) 157-167.

[25] N. Woudstra, T. Woudstra, A. Pirone, T.v.d. Stelt, Thermodynamic evaluation of combined cycle plants, Energy Conversion and Management, 51 (2010) 1099-1110.

[26] M. Granovskii, I. Dincer, M.A. Rosen, Performance comparison of two combined SOFC–gas turbine systems, Journal of Power Sources, 165 (2007) 307-314.

[27] A. Arsalis, Thermoeconomic modeling and parametric study of hybrid SOFC–gas turbine–steam turbine power plants ranging from 1.5 to 10 MWe, Journal of Power Sources, 181 (2008) 313-326.

[28] A. Shirazi, M. Aminyavari, B. Najafi, F. Rinaldi, M. Razaghi, Thermal–economic–environmental analysis and multi-objective optimization of an internal-reforming solid oxide fuel cell–gas turbine hybrid system, International Journal of Hydrogen Energy, 37 (2012) 19111-19124.

[29] S.H. Chan, K.A. Khor, Z.T. Xia, A complete polarization model of a solid oxide fuel cell and its sensitivity to the change of cell component thickness, Journal of Power Sources, 93 (2001) 130-140.

[30] P.G. Bavarsad, Energy and exergy analysis of internal reforming solid oxide fuel cell–gas turbine hybrid system, International Journal of Hydrogen Energy, 32 (2007) 4591-4599.

[31] S. Motahar, A.A. Alemrajabi, Exergy based performance analysis of a solid oxide fuel cell and steam injected gas turbine hybrid power system, International Journal of Hydrogen Energy, 34 (2009) 2396-2407.

[32] A.V. Akkaya, B. Sahin, H. Huseyin Erdem, An analysis of SOFC/GT CHP system based on exergetic performance criteria, International Journal of Hydrogen Energy, 33 (2008) 2566-2577.

[33] A. Shirazi, S. Pintaldi, S.D. White, G.L. Morrison, G. Rosengarten, R.A. Taylor, Solar-assisted absorption air-conditioning systems in buildings: Control strategies and operational modes, Applied Thermal Engineering, 92 (2016) 246-260.

[34] A.F. Massardo, Internal Reforming Solid Oxide Fuel Cell Gas Turbine Combined Cycles (IRSOFC-GT)—Part II: Exergy and Thermoeconomic Analyses, Journal of Engineering for Gas Turbines and Power, 125 (2002) 67-74.

[35] A.H. Mamaghani, B. Najafi, A. Shirazi, F. Rinaldi, Exergetic, economic, and environmental evaluations and multi-objective optimization of a combined molten carbonate fuel cell-gas turbine system, Applied Thermal Engineering, 77 (2015) 1-11.

[36] A. Shirazi, R.A. Taylor, S.D. White, G.L. Morrison, A systematic parametric study and feasibility assessment of solar-assisted single-effect, double-effect, and triple-effect absorption chillers for heating and cooling applications, Energy Conversion and Management, 114 (2016) 258-277.

[37] D.F. Cheddie, Thermo-economic optimization of an indirectly coupled solid oxide fuel cell/gas turbine hybrid power plant, International Journal of Hydrogen Energy, 36 (2011) 1702-1709.

[38] F. Calise, A. Palombo, L. Vanoli, Design and partial load exergy analysis of hybrid SOFC–GT power plant, Journal of Power Sources, 158 (2006) 225-244.

[39] F. Calise, M. Dentice d' Accadia, L. Vanoli, M.R. von Spakovsky, Single-level optimization of a hybrid SOFC–GT power plant, Journal of Power Sources, 159 (2006) 1169-1185.

[40] P.K. Sahoo, Exergoeconomic analysis and optimization of a cogeneration system using evolutionary programming, Applied Thermal Engineering, 28 (2008) 1580-1588.

[41] H. Sayyaadi, Multi-objective approach in thermoenvironomic optimization of a benchmark cogeneration system, Applied Energy, 86 (2009) 867-879.

[42] M.V.J.J. Suresh, K.S. Reddy, A.K. Kolar, 3-E analysis of advanced power plants based on high ash coal, International Journal of Energy Research, 34 (2010) 716-735.

[43] N. Autissier, F. Palazzi, F. Marechal, J. van Herle, D. Favrat, Thermo-Economic Optimization of a Solid Oxide Fuel Cell, Gas Turbine Hybrid System, Journal of Fuel Cell Science and Technology, 4 (2006) 123-129.

[44] F. Palazzi, N. Autissier, F.M.A. Marechal, D. Favrat, A methodology for thermo-economic modeling and optimization of solid oxide fuel cell systems, Applied Thermal Engineering, 27 (2007) 2703-2712.

[45] S. Sanaye, A. Katebi, 4E analysis and multi objective optimization of a micro gas turbine and solid oxide fuel cell hybrid combined heat and power system, Journal of Power Sources, 247 (2014) 294-306.

[46] B. Najafi, A. Shirazi, M. Aminyavari, F. Rinaldi, R.A. Taylor, Exergetic, economic and environmental analyses and multi-objective optimization of an SOFC-gas turbine hybrid cycle coupled with an MSF desalination system, Desalination, 334 (2014) 46-59.

[47] M. Canavar, A. Mat, S. Celik, B. Timurkutluk, Y. Kaplan, Investigation of temperature distribution and performance of SOFC short stack with/without machined gas channels, International Journal of Hydrogen Energy, 41 (2016) 10030-10036.

[48] T. Choudhary, Sanjay, Computational analysis of IR-SOFC: Transient, thermal stress, carbon deposition and flow dependency, International Journal of Hydrogen Energy, 41 (2016) 10212-10227.

[49] N.S. Siefert, S. Litster, Exergy & economic analysis of biogas fueled solid oxide fuel cell systems, Journal of Power Sources, 272 (2014) 386-397.

[50] S. Sanaye, A. Shirazi, Four E analysis and multi-objective optimization of an ice thermal energy storage for air-conditioning applications, International Journal of Refrigeration, 36 (2013) 828-841.

[51] M. Navidbakhsh, A. Shirazi, S. Sanaye, Four E analysis and multi-objective optimization of an ice storage system incorporating PCM as the partial cold storage for air-conditioning applications, Applied Thermal Engineering, 58 (2013) 30-41.

[52] I. Fuel cell handbook. 7th ed. Morgantown: WV: EG&G Technical Services, in, Science Applications International Corporation, 2004.

[53] S.H. Chan, H.K. Ho, Y. Tian, Modelling of simple hybrid solid oxide fuel cell and gas turbine power plant, J. Power Sources, 109 (2002) 111-120.

[54] N.F. Bessette II, W.J. Wepfer, Electrochemical and thermal simulation of a solid oxide fuel cell, Chem. Eng. Commun., 147 (1996) 1-15.

[55] A. Shirazi, R.A. Taylor, S.D. White, G.L. Morrison, Transient simulation and parametric study of solar-assisted heating and cooling absorption systems: An energetic, economic and environmental (3E) assessment, Renewable Energy, 86 (2016) 955-971.

[56] S.H. Chan, C.F. Low, O.L. Ding, Energy and exergy analysis of simple solid-oxide fuel-cell power systems, J. Power Sources, 103 (2002) 188-200.

[57] S. Kakaç, H. Liu, Heat Exchangers: Selection, Rating, and Thermal Design, Second Edition, CRC Press, 2002.

[58] P. Ahmadi, I. Dincer, Thermodynamic analysis and thermoeconomic optimization of a dual pressure combined cycle power plant with a supplementary firing unit, Energy Conversion and Management, 52 (2011) 2296-2308.

[59] S. Pelster, Environomic Modeling & Optimization of Advanced Combined Cycle Cogeneration Power Plants Including CO2 Separation Options, in, Vol. Doctoral Thesis, Ecole Polytechnique Federale de Lausanne, Lausanne, Switzerland, 1998.

[60] B. Oyarzabal, Application of a Decomposition Strategy to the Optimal Synthesis/Design of a Fuel Cell Sub-system, in: Department of Mechanical Engineering, Vol. M.S. Thesis, Virginia Polytechnic Institute & State University, Blacksburg, VA, 2001.

[61] P. Roosen, S. Uhlenbruck, K. Lucas, Pareto optimization of a combined cycle power system as a decision support tool for trading off investment vs. operating costs, International Journal of Thermal Sciences, 42 (2003) 553-560.

[62] Q. Li, A. Shirazi, C. Zheng, G. Rosengarten, J.A. Scott, R.A. Taylor, Energy concentration limits in solar thermal heating applications, Energy, 96 (2016) 253-267.

[63] A. Traverso, A.F. Massardo, W. Cazzola, G. Lagorio, WIDGET-TEMP: A Novel Web-Based Approach for Thermoeconomic Analysis and Optimization of Conventional and Innovative Cycles, ASME transactions, (2004).

[64] R.F. Boehm, Design analysis of thermal systems, Wiley, 1987.

[65] I.R.A.f.E.G.a. Water, http://www.autorita.energia.it/, (2015).

[66] A. Lazzaretto, A. Toffolo, Energy, economy and environment as objectives in multi-criterion optimization of thermal systems design, Energy, 29 (2004) 1139-1157.

[67] B. Najafi, H. Najafi, M. Idalik, Computational fluid dynamics investigation and multi-objective optimization of an engine air-cooling system using genetic algorithm, Proceedings of the Institution of Mechanical Engineers, Part C: Journal of Mechanical Engineering Science, 225 (2011) 1389-1398.

[68] A. Shirazi, B. Najafi, M. Aminyavari, F. Rinaldi, R.A. Taylor, Thermal–economic–environmental analysis and multi-objective optimization of an ice thermal energy storage system for gas turbine cycle inlet air cooling, Energy, 69 (2014) 212-226.

[69] I.C. Bank, URL: https://www.bancaditalia.it, (accessed January 2015), (2015).

[70] M. Aminyavari, B. Najafi, A. Shirazi, F. Rinaldi, Exergetic, economic and environmental (3E) analyses, and multi-objective optimization of a CO2/NH3 cascade refrigeration system, Applied Thermal Engineering, 65 (2014) 42-50.

[71] Z. Yue, A method for group decision-making based on determining weights of decision makers using TOPSIS, Applied Mathematical Modelling, 35 (2011) 1926-1936.

Figure Captions

Fig. 1. Schematic diagram of the SOFC-GT cycle coupled with a Rankine bottoming cycle

Fig. 2. Flowchart of genetic algorithm technique for system optimization

Fig. 3. Comparison between the current density-cell voltage curve generated by the results of the present model and the data from a previous study [29]

Fig. 4. Pareto optimal frontier obtained from multi-objective optimization of the system

Fig. 5. The set of non-dimensional Pareto optimal solutions using TOPSIS decision-making method to specify the final optimal design point of the system

Fig. 6. Exergy destruction rate in the major components of the system at three different optimal design points

Fig. 7. Annual power enhancement and CO_2 emissions saved by integration of a Rankine bottoming cycle to the SOFC-GT plant

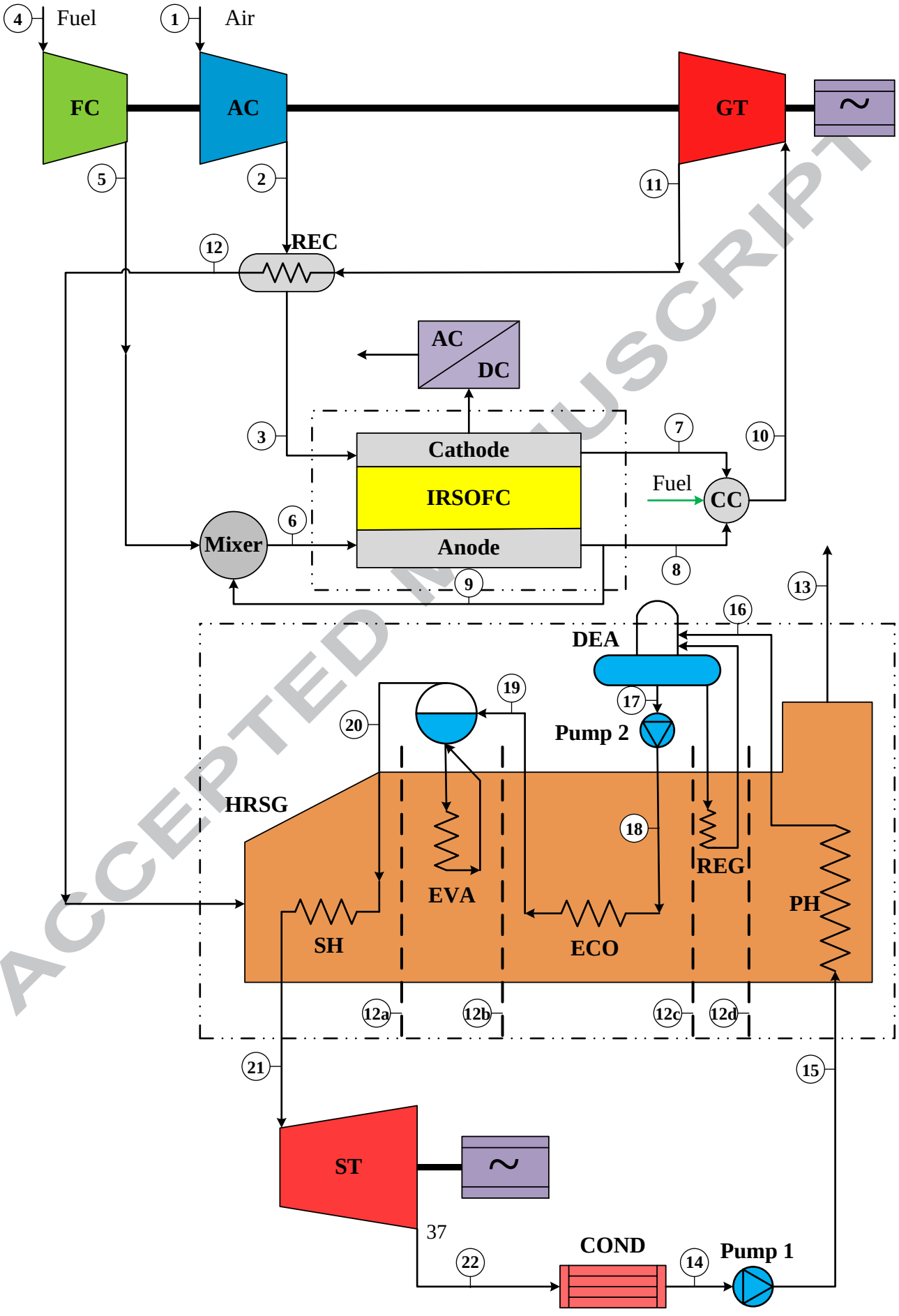

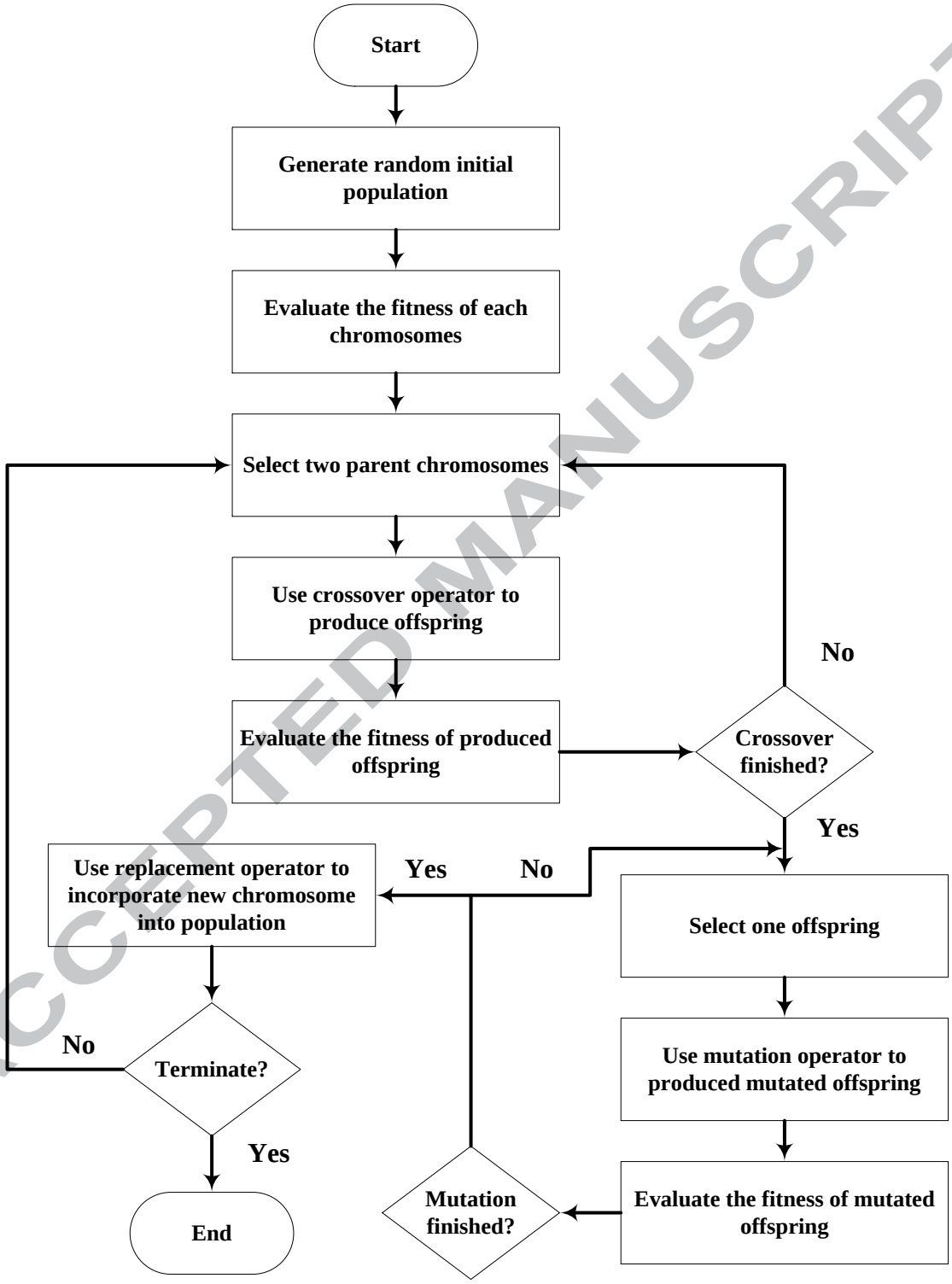

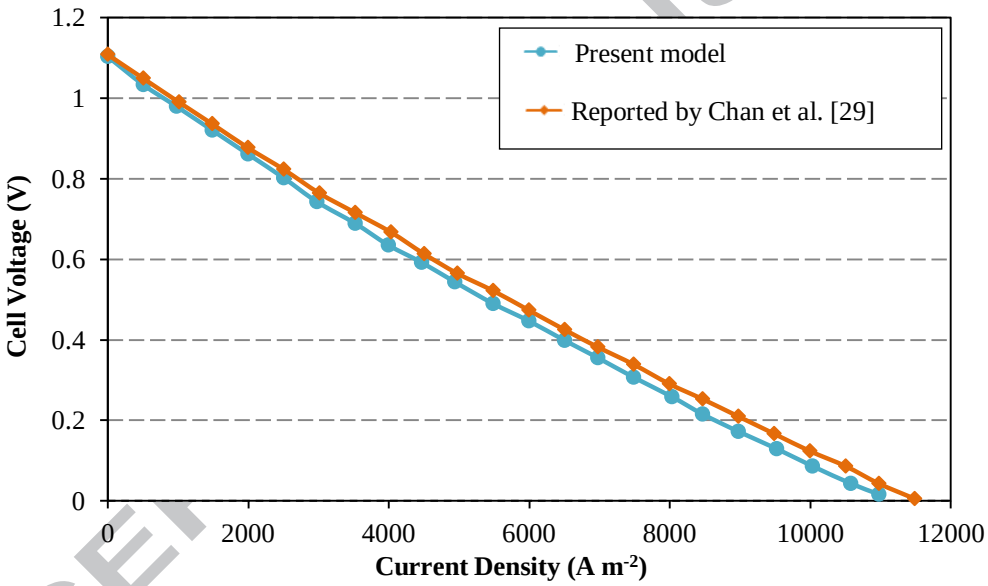

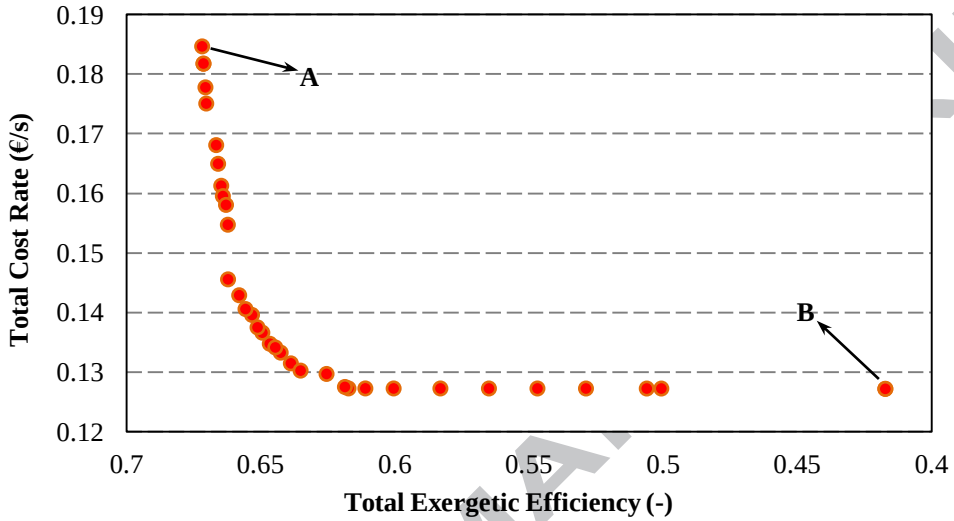

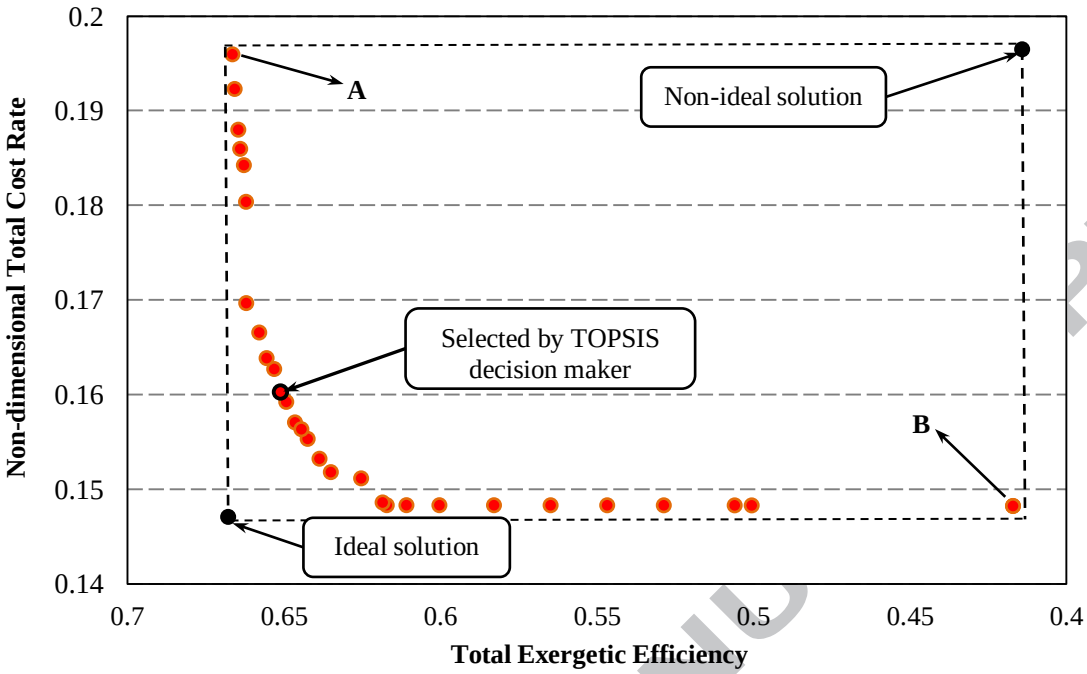

Point A as an extreme in favor of exergetic efficiency

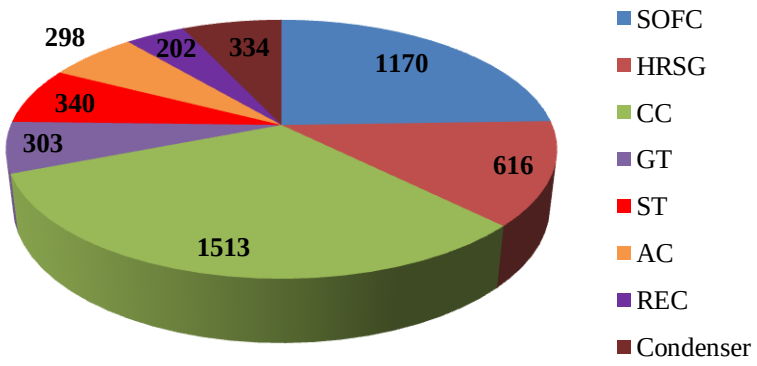

Point B as an extreme in favor of total cost rate

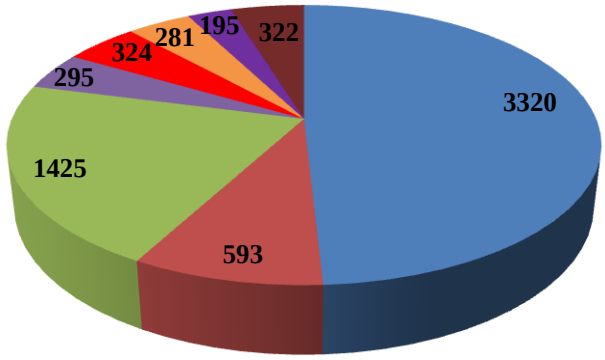

Multi objective optimization (trade-off approach)

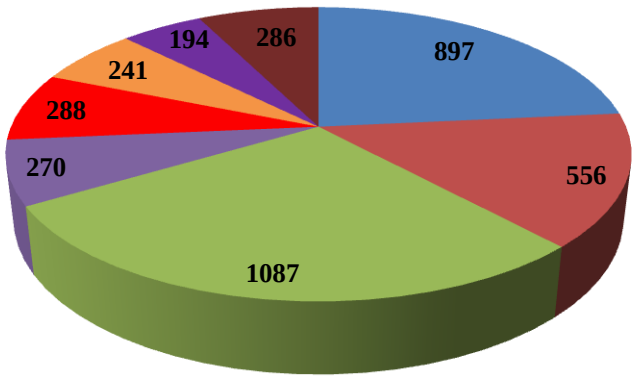

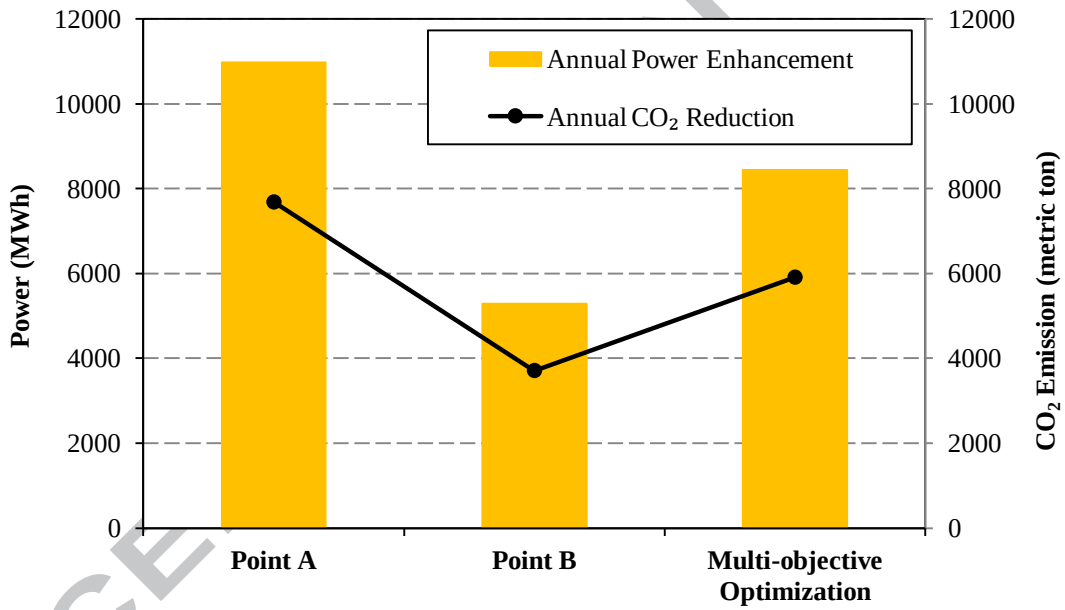

Table 1
The exergy destruction rate for each component of the plant

Component	Exergy destruction rate
Air compressor	$\dot{E}_{D,AC} = \dot{E}_1 - \dot{E}_2 + \dot{W}_{AC}$
Fuel compressor	$\dot{E}_{D,FC} = \dot{E}_4 - \dot{E}_5 + \dot{W}_{FC}$
SOFC	$\dot{E}_{D,SOFC} = \dot{E}^{Q}_{SOFC} - \dot{E}^{W}_{SOFC} + \left(\dot{E}_3 + \dot{E}_6\right) - \left(\dot{E}_7 + \dot{E}_8\right) = -\dot{Q}_{l,SOFC}\left(1 - \frac{T_0}{T_{SOFC}}\right) - \dot{W}_{SOFC,DC} + \left(\dot{E}_3 + \dot{E}_6\right) - \left(\dot{E}_7 + \dot{E}_8\right)$
Combustion chamber	$\dot{E}_{D,CC} = \dot{E}^{Q}_{CC} + \left(\dot{E}_7 + \dot{E}_8\right) - \dot{E}_{10} = -\dot{Q}_{l,CC}\left(1 - \frac{T_0}{T_{CC}}\right) + \left(\dot{E}_7 + \dot{E}_8\right) - \dot{E}_{10}$
Gas turbine	$\dot{E}_{D,GT} = \dot{E}_9 - \dot{E}_{10} - \dot{W}_{GT}$
Recuperator	$\dot{E}_{D,REC} = \left(\dot{E}_2 + \dot{E}_{11}\right) - \left(\dot{E}_3 + \dot{E}_{12}\right)$
Mixer	$\dot{E}_{D,mixer} = \dot{E}_5 + \dot{E}_9 - \dot{E}_6$
Water pump	$\dot{E}_{D,pump1} = \dot{E}_{14} - \dot{E}_{15} + \dot{W}_{pump1}$
HRSG	$\dot{E}_{D,HRSG} = \left(\dot{E}_{12} - \dot{E}_{13}\right) + \left(\dot{E}_{15} - \dot{E}_{21}\right) + \dot{W}_{pump2}$
Steam turbine	$\dot{E}_{D,ST} = \dot{E}_{21} - \dot{E}_{22} - \dot{W}_{ST}$
Condenser	$\dot{E}_{D,COND} = \left(\frac{T_0}{T_{COND}} - 1\right)\dot{Q}_{COND} + \left(\dot{E}_{22} - \dot{E}_{14}\right)$

Table 2
Capital cost function of various components in the plant [7, 52, 56-61]

System component	Capital cost function
Compressor	$Z_C = \frac{39.5 \times \dot{m}}{0.9 - \eta_C}\left(\frac{p_{dc}}{p_{suc}}\right)\ln\left(\frac{p_{dc}}{p_{suc}}\right)$
Combustion Chamber	$Z_{CC} = \left(\frac{46.08 \times \dot{m}_{in}}{0.995 - \frac{p_{out}}{p_{in}}}\right)\left[1 + \exp\left(0.018T_{out} - 26.4\right)\right]$
Gas turbine	$Z_{GT} = \dot{W}_T\left[1318.5 - 98.328\ln\left(\dot{W}_T\right)\right]$
Steam turbine	$Z_{ST} = 3744.3\left(\dot{W}_{ST}\right)^{0.7} - 61.3\left(\dot{W}_{ST}\right)^{0.95}$
Generator	$Z_{Generator} = 26.18\left(\dot{W}_T\right)^{0.95}$
Recuperator	$Z_{REC} = 2290A_{REC}^{0.6}$
SOFC stack	$Z_{SOFC} = A_{SOFC}\left(2.96T_{SOFC} - 1907\right)$
Auxiliary devices	$Z_{SOFC,aux} = 0.1\left(Z_{SOFC}\right)$
Pump	$Z_{PUMP} = 705.48 \times \dot{W}_{pump}^{0.71}\left(1 + \frac{0.2}{1 - \eta_{pump}}\right)$
Inverter	$Z_{Inverter} = 10^5\left(\frac{\dot{W}_{SOFC,DC}}{500}\right)^{0.7}$
HRSG	$Z_{HRSG} = c_{41}\left(\sum_i\left(f_{p,i} \times f_{T,steam,i} \times f_{T,gas,i}\right)\left(\frac{\dot{Q}_i}{\Delta T_{ln,i}}\right)^{0.8}\right) + c_{42}\sum_i f_{p,i}\dot{m}_{steam,i} + c_{43}\dot{m}_{gas}^{1.2}$

Table 3
List of constraints for system optimization and the range of variation of design parameters

Constraint	**Reason**
$2 < r_{p,\,AC} < 16$	For typical technology and commercial availability
$1000 < i < 7000$	Minimum and maximum values of cell current density
$0.1 < U_a < 0.7$	Minimum and maximum values of air utilization factor
$0.5 < U_f < 0.9$	Minimum and maximum values of fuel utilization factor
$2 < S/C < 4$	Minimum and maximum values of steam to carbon ratio
$10<P_{eva}<25$	Minimum and maximum values of evaporation pressure
$TIT < 1550$ K	Material temperature limit
$T_{SOFC} < 1400$ K	Material temperature limit
$T_{stack} > 374$ K	To avoid formation of carbonic acid in the exhaust gas

Table 4
Input parameters used for simulation of the cogeneration system [28]

Parameter	Value
Fuel compressor isentropic efficiency (η_{FC})	0.82
Air compressor isentropic efficiency (η_{AC})	0.80
Gas turbine isentropic efficiency (η_{GT})	0.80
Recuperator effectiveness	0.88
Combustion chamber efficiency (η_{CC})	0.98
Electric generator efficiency (η_{G})	0.95
Pump efficiency (η_{P})	0.83
DC-AC inverter efficiency ($\eta_{Inverter}$)	0.95
SOFC heat loss (% of MW_{DC})	1.7
Pressure losses	
Recuperator (%)	4
Fuel cell stack (%)	4
Combustion chamber (%)	5
Fuel properties	
Composition (% volume)	CH_4 (95%), C_2H_6 (2.5%), CO_2 (1%), N_2 (1.5%)
LHV (kJ kg^{-1})	45,100
Specific chemical exergy (kJ kg^{-1})	45,713
Air properties	
Composition (% volume)	N_2 (79%), O_2 (21%)
Molar weight (kg $kmol^{-1}$)	28.97

Table 5
Design parameters used for simulation of HRSG [58]

HRSG Parameter	Value
Pressure (bar)	
Condenser	0.05
Regenerator	2
Pressure losses	
Superheater	7 (% inlet pressure)
Economizer 1	10 (% inlet pressure)
Economizer 2	10 (% inlet pressure)
Heat loss of HRSG	0.005
Approach point temperature (K)	10
Pinch point temperature (K)	5
Subcooling temperature (K)	2
Hydraulic efficiency of feed water pump	0.83
Hydraulic efficiency of condenser	0.85
Mechanical/Electrical efficiency	0.975
Mechanical efficiency of turbine	0.995
Electrical efficiency of turbine	0.985

Table 6
Stream data of the hybrid plant at the base operating condition

Node	T(K)	P(bar)	h (kJ/kg)	s (kJ/kg)
1	288.0	1.00	288.2	6.83
2	575.5	8.00	581.7	6.94
3	900.0	7.76	933.9	7.43
4	288.0	1.00	887.4	6.60
5	485.8	8.00	1379.5	6.81
6	909.8	8.00	2480.6	3.91
7	1017.5	7.14	1082.3	7.63
8	1017.5	7.36	4609.8	15.33
9	1017.5	7.36	4609.8	15.33
10	1598.2	7.14	2091.7	8.11
11	1174.8	1.18	1528.9	8.24
12	915.4	1.14	1201.5	7.93
13	380.0	1.03	574.0	6.93
14	306.0	0.05	137.7	0.48
15	306.0	2.22	138.0	0.48
16	391.4	2.00	496.2	1.51
17	393.4	2.00	504.7	1.53
18	393.6	22.22	507.3	1.53
19	483.5	20.00	899.4	2.43
20	485.5	20.00	2798.3	6.34

21	905.4	18.60	3764.5	7.82
22	358.9	0.05	2661.1	8.70

Table 7

Optimal design parameters of the system obtained from three optimization standpoints

Design parameter	**Point A as an extreme in favor of exergetic efficiency**	**Point B as an extreme in favor of total cost rate**	**Multi objective optimization (trade-off approach)**
$r_{p,AC}$	9.99	9.45	9.90
i (A/m^2)	2312	4443	3103
U_a	0.49	0.49	0.49
U_f	0.89	0.60	0.61
S/C ratio	1.86	1.81	1.82
P_{eva}	21.2	22.0	21.7

Table 8
Capital costs of the major components of the system (in terms of million Euro)

Component	Point A as an extreme in favor of exergetic efficiency	Point B as an extreme in favor of total cost rate	Multi objective optimization (trade-off approach)
Air Compressor	0.047846	0.026	0.036769
Fuel Compressor	0.001485	0.001369	0.001469
Gas turbine	1.673846	1.002308	1.36
Steam turbine	0.406923	0.249231	0.341538
Recuperator	0.069577	0.046385	0.057154
Condenser	0.030615	0.017923	0.024385
SOFC stack	3.275385	1.131538	1.901538
Pump	0.002538	0.002631	0.002608
HRSG	0.401538	0.219231	0.322308

Table 9
The hybrid system performance-related results obtained from three optimization standpoints

Parameter	Point A as an extreme in favor of exergetic efficiency	Point B as an extreme in favor of total cost rate	Multi objective optimization (trade-off approach)
SOFC temperature (K)	960.7	1000.3	962.3
Social cost of air pollution (M Euro year $^{-1}$)	0.4877	0.1554	0.3946
Compressor electrical power (kW)	2457.7	1451.0	1931.6
Power output from the SOFC (kW)	7545.9	3613.4	5282.6
Power output from the GT (kW)	4345.8	2309.9	3357.9

Power output from the ST (kW)	1371.4	661.99	1054.9
Net electrical power output (MW)	10.801	5.132	7.761
Total exergetic efficiency (%)	67.18	41.71	65.11
Net electrical efficiency (%)	69.12	42.81	66.86
Total annual cost (M Euro)	5.3191	3.6617	3.9586

Highlights

- An exergetic-economic-environmental analysis of an SOFC-GT-ST plant was performed
- Exergetic efficiency and total cost rate of the plant were considered as objectives
- Multi-objective optimization was conducted to obtain a set of optimal solutions
- Exergy destruction rate and capital cost of components of the plant were determined
- The Rankine bottoming cycle enhanced the exergetic efficiency of the plant by 8.84%